Human Molecular Genetics, 2010, Vol. 19, No. 20 ***4043–4058***
doi:10.1093/hmg/ddq322
Advance Access published on July 28, 2010

Modulation of energy deficiency in Huntington's disease via activation of the peroxisome proliferator-activated receptor gamma

Ming-Chang Chiang[1,2], Chiung-Mei Chen[3], Maw-Rong Lee[4], Hsiao-Wen Chen[2], Hui-Mei Chen[1], Yu-Shuo Wu[1], Cheng-Han Hung[4], Jheng-Jie Kang[1], Ching-Pang Chang[1], Chen Chang[1], Yih-Ru Wu[3], Yau-Sheng Tsai[5] and Yijuang Chern[1,*]

[1]Institute of Biomedical Sciences, Academia Sinica, Nankang, Taipei 115, Taiwan, [2]Graduate Institute of Biotechnology, Chinese Culture University, Taipei 111, Taiwan, [3]Department of Neurology, Chang Gung Memorial Hospital, Linkou Medical Center and College of Medicine, Chang-Gung University, Taoyuan 333, Taiwan, [4]Department of Chemistry, National Chung-Hsing University, Taichung 402, Taiwan and [5]Institute of Clinical Medicine, College of Medicine, National Cheng Kung University, Tainan 701, Taiwan

Received June 24, 2010; Revised and Accepted July 22, 2010

Huntington's disease (HD) is a neurodegenerative disease caused by the expansion of a CAG trinucleotide repeat in exon 1 of the huntingtin (*HTT*) gene. Here, we report that the transcript of the peroxisome proliferator-activated receptor-γ (PPARγ), a transcription factor that is critical for energy homeostasis, was markedly downregulated in multiple tissues of a mouse model (R6/2) of HD and in lymphocytes of HD patients. Therefore, downregulation of PPARγ seems to be a pathomechanism of HD. Chronic treatment of R6/2 mice with an agonist of PPARγ (thiazolidinedione, TZD) rescued progressive weight loss, motor deterioration, formation of mutant Htt aggregates, jeopardized global ubiquitination profiles, reduced expression of two neuroprotective proteins (brain-derived neurotrophic factor and Bcl-2) and shortened life span exhibited by these mice. By reducing HTT aggregates and, thus, ameliorating the recruitment of PPARγ into HTT aggregates, chronic TZD treatment also elevated the availability of the PPARγ protein and subsequently normalized the expression of two of its downstream genes (the glucose transporter type 4 and PPARγ coactivator-1 alpha genes). The protective effects described above appear to have been exerted, at least partially, via direct activation of PPARγ in the brain, as TZD was detected in the brains of mice treated with TZD and because a PPARγ agonist (rosiglitazone) protected striatal cells from mHTT-evoked energy deficiency and toxicity. We demonstrated that the systematic downregulation of PPARγ seems to play a critical role in the dysregulation of energy homeostasis observed in HD, and that PPARγ is a potential therapeutic target for this disease.

INTRODUCTION

Huntington's disease (HD) is an autosomal-dominant neurodegenerative disease characterized by chorea, dementia and psychiatric symptoms. The causative mutation is the expansion of a CAG trinucleotide repeat in exon 1 of the huntingtin (*HTT*) gene (1). The major characteristic of HD is the region-specific degeneration of neurons in the striatum and cortex, which leads to a movement disorder and dementia (2). The hallmark of HD is the formation of HTT aggregates in the nucleus of affected neurons of human patients and HD mice because of insufficient protein degradation (3,4). Accumulation of HTT aggregates jeopardizes the functions of many proteins, including components of protein-folding and proteolytic machineries, by recruiting these proteins into HTT aggregates, and thus reducing their normal availability (5,6).

*To whom correspondence should be addressed at: Institute of Biomedical Sciences, Academia Sinica, Taipei 11529, Taiwan. Tel: +886 226523913; Fax: +886 227829143; Email: bmychern@ibms.sinica.edu.tw

Aberrant transcriptional regulation is one of the major pathogenic mechanisms underlying the toxicity induced by mutant HTT (mHTT), as cleaved mHTT binds to various transcription factors and/or coactivators (such as p53, Sp1, TAFII130, and the CREB-binding protein) and interferes with their functions (7–10).

Deficits in energy metabolism are also important clinical presentations of HD. Abnormal metabolic profiles (such as hyperglycemia, deficient urea-cycle activity and disturbed cholesterol biosynthesis) were reported in several HD mouse models and in HD patients (10–14). We showed previously that the expression of mHTT suppresses the function of C/EBPα (10), a transcription factor that is critical for energy homeostasis (15). Among the downstream target genes of C/EBPα, the peroxisome proliferator-activated receptor-γ (PPARγ) attracted our attention because of its implication in energy metabolism. Given the importance of PPARγ, alteration of its expression may contribute to the dysregulation of the energy metabolism and low body weight observed in HD. An earlier study showed that the expression of mHTT suppresses the transcriptional activity of PPARγ and results in mitochondrial dysfunction in a striatal cell line (16). Thus, we set out to evaluate the expression and activity of PPARγ systematically in a transgenic mouse model of HD [R6/2 (17)] and in lymphocytes of HD patients. To assess the functional importance of the altered expression of PPARγ in HD, we treated R6/2 mice with a well-characterized agonist of PPARγ (thiazolidinedione, TZD) and assessed its potential beneficial effects on the progression of HD. The results presented here show that the expression of PPARγ was attenuated in the brain and in two peripheral tissues (the liver and adipocytes) of these animals via the use of at least two different pathways. The level of PPARγ was also decreased in lymphocytes of HD patients, which suggests its clinical relevance in HD. Treatment with TZD, which activates PPARγ-mediated pathways, resulted in beneficial effects on the energy deficiency exhibited by, and on several major phenotypes of, R6/2 mice. Our study showed clearly that PPARγ deficiency in the entire body may be an authentic contributor to HD pathogenesis and represents a potential drug target that is worthy of further evaluation in this disease.

RESULTS

To evaluate whether the expression and function of PPARγ are jeopardized in HD, we first assessed the level of the PPARγ transcript in several tissues known to be affected in R6/2 mice. Using a quantitative polymerase chain reaction (qPCR) method, we demonstrated that the levels of the PPARγ transcript in the striatum, the liver, subcutaneous white adipocytes (WATs), and abdominal WATs of R6/2 mice were significantly lower than those observed in wild-type (WT) mice (Fig. 1A–D).To determine whether lower PPARγ expression also occurs in human HD patients, we performed a pilot study to assess the levels of the PPARγ transcript in lymphocytes of 17 HD patients and 18 age-matched healthy volunteers (Table 1). In accordance with the findings from R6/2 mice, the level of the PPARγ transcript in lymphocytes of HD patients was lower than that detected in age-matched controls (Fig. 1E). Next, we investigated whether the function of PPARγ was also affected by mHTT using a *PPRE-Luc* reporter gene, which contains a PPAR response element [*PPRE* (18)]. Binding of PPARγ to the *PPRE* element leads to the expression of the LUC reporter protein. Compared with what was observed in cells transfected with a control construct (Q_{25}-HTT), expression of polyQ-expanded mHTT (Q_{158}-HTT) in a striatal cell line (ST14A) inhibited the expression of the LUC reporter markedly, which indicates that mHTT inhibited the function of PPARγ (Fig. 1F). Activation of PPARγ using an agonist (rosiglitazone, Rosi) increased the expression of the LUC reporter, which was repressed by mHTT. This rescue effect of Rosi was blocked effectively by an antagonist of PPARγ (GW9662), demonstrating that the action of Rosi was mediated by PPARγ (Fig. 1F). Together, these data suggest that inhibition of PPARγ by mHTT occurs in the central nervous system (CNS) and in several peripheral tissues, and that it is an important pathogenic feature of HD.

To rescue the downregulation of PPARγ in HD, we treated R6/2 mice with a well-characterized PPARγ agonist (TZD) to activate its function, and evaluated disease progression. Starting at 4 weeks of age, R6/2 mice were fed a diet supplemented with four different TZD dosages (0.001, 0.05, 0.01 and 0.02%) for 8 weeks. Data analyses of body weight and rotarod performance indicated that the 0.01% TZD dietary supplement was most effective (Supplementary Material, Fig. S1). Therefore, we chose to treat R6/2 mice with a dietary supplement of 0.01% TZD in all further analyses. Because PPARγ regulates its own expression at the transcriptional level (19), R6/2 mice that were fed a TZD-supplemented diet exhibited elevated levels of the PPARγ transcript in all tissues tested (Fig. 1A–D). In addition, R6/2 mice that were fed a TZD-supplemented diet had a higher body weight compared with animals that were fed the control diet (Fig. 2A). With the exception of the first 2 weeks of this diet, during which TZD increased the food intake by ∼20%, chronic TZD treatment did not affect the daily food intake (data not shown). Thus, the increase in body weight after TZD treatment is likely to have resulted from an ameliorated energy homeostasis and not from a change in appetite. In addition to the increase in body weight, chronic TZD administration also markedly rescued the dysregulated energy storage in the brown adipose tissue mass and alterations in the lipogenesis of WATs, which confirmed the efficacy of TZD administration (Table 2).

Studies from various laboratories, including our own, demonstrated that a subpopulation of HD patients and several HD mouse models exhibit hyperglycemia and insulin resistance (12,20–22). Importantly, amelioration of hyperglycemia is associated with improvement of the neurological deficits of HD (21). As TZD is a well-known insulin sensitizer (23), we performed experiments aimed at examining whether chronic TZD supplementation normalized the blood glucose levels of R6/2 mice. Consistent with earlier reports (24,25), an increase of ∼1-fold in the levels of blood glucose was found in R6/2 mice at the age of 8 weeks compared with WT mice. Chronic treatment with TZD greatly reduced the elevated level of blood glucose in R6/2 mice, without affecting the plasma level of insulin (Fig. 2B, Table 3),

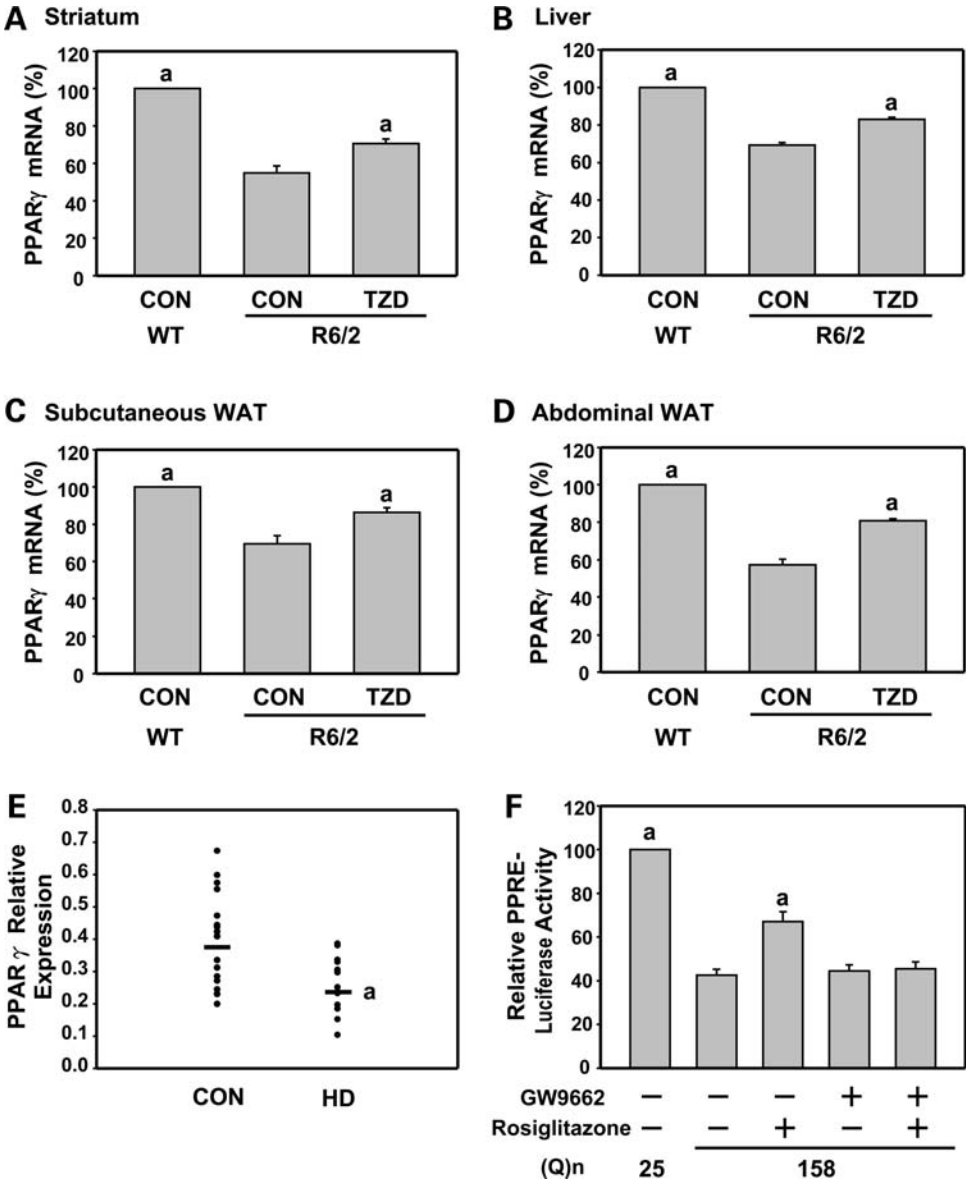

Figure 1. Chronic TZD elevated the reduced PPARγ expression in multiple tissues expressing mHtt, and enhanced the transcriptional function of PPARγ. Mice were fed the control or 0.01% TZD-supplemented diet from the age of 4 weeks. For the indicated mice, striatal (**A**; 12 weeks old), liver (**B**; 12 weeks old), subcutaneous white adipose tissue (WAT) (**C**; 10.5 weeks old) and abdominal WAT (**D**; 10.5 weeks old) were collected to determine the transcript levels of PPARγ using a quantitative RT–PCR technique. Expression levels of PPARγ were normalized to that of GAPDH or HPRT. Data are presented as the mean ± SEM from three independent experiments. [a]Specific comparison to HD mice fed the control diet ($P < 0.05$; one-way ANOVA). (**E**) Leukocyte samples were collected from 18 control subjects (CON) and 17 HD patients (HD) to measure PPARγ expression by a quantitative RT–PCR technique. The expression levels of PPARγ were normalized to that of GAPDH. [a]The specific comparison with control subjects (CON) ($P < 0.05$; one-way ANOVA). (**F**) The indicated Htt construct was cotransfected with a PPAR response element (PPRE) promoter construct into ST14A cells for 24 h, and then treated with the indicated reagents (10 μM Rosi or 20 μM GW9662) for another 48 h. The luciferase activity of each construct was measured and normalized to the protein content. Values are expressed as percentages of the promoter activity of the PPRE construct in the presence of pcDNA3-(Htt-$(Q)_{25}$) under control conditions (no treatment) and represent the mean ± SEM of at least three determinations. [a]Specific comparison between the indicated group and that transfected with pcDNA3.1-$(Q)_{158}$-Htt with no treatment ($P < 0.05$; one-way ANOVA).

which demonstrated the effect of TZD on glucose regulation. We did not detect a significant effect of TZD on the steady-state levels of two plasma lipid parameters (triglycerides and free fatty acids) in R6/2 mice (Table 3). Most importantly, R6/2 mice that were fed the TZD diet exhibited a significant improvement of motor coordination, as assessed by rotarod performance (Fig. 2C). In addition, R6/2 mice that were fed TZD diet showed reduced hind-limb clasping, which is a sign of motor impairment in HD mice (26), compared with animals that were fed the control diet (Fig. 2D). Motor functions were also assessed using a CatWalk gait automatic analyzer (Fig. 2E). Compared with WT mice, R6/2 mice at the age of 12 weeks showed gait disturbances that manifested as a shorter stride. Chronic TZD supplementation normalized the shortened stride length of R6/2 mice (Fig. 2E). Moreover, the life span of R6/2 mice treated with 0.01%

Table 1. Clinical characteristics of the Huntington's disease patients and healthy volunteers

Parameters	Controls ($n = 18$)	HD patients ($n = 17$)
Gender (male/female)	11/7	11/6
Age (years)	51.00 ± 2.94	50.41 ± 3.12
Age at symptom onset (years)		43.07 ± 2.98
Disease duration (years)		5.00 ± 1.13
Expanded CAG repeat No.		44.18 ± 1.49
UHDRS		
Motor score		26.35 ± 5.40
Independence scale		79.41 ± 5.39
Total functional capacity		10.00 ± 0.85

Values are expressed as the mean ± SEM. UHDRS denotes the Unified Huntington's Disease Rating Scale. Scale ranges (normal to most severe) include a total motor score (0 ~ 124), independence score (100 ~ 10), and total functional capacity (13 ~ 0).

TZD was longer compared with animals that were fed the control diet (Fig. 2F).

Next, we dissected the molecular mechanisms underlying the beneficial effects of TZD in R6/2 mice. First, we assessed the actions of chronic TZD administration in adipocytes of R6/2 mice, as TZD effectively ameliorated lipogenesis in these mice (Table 2). The mechanism underlying this phenomenon is of great interest because reduced PPARγ activity in adipose tissues causes progressive loss of fat (27), which is very similar to the adipose tissue dysfunction found in HD (28–30). As predicted, the expression of two downstream target genes of PPARγ [the PPAR coactivator-1α (*PGC-1α*) (31) and glucose transporter 4 (*Glut4*) (32) genes] was significantly altered in the subcutaneous and abdominal WATs of R6/2 mice. Chronic treatment with TZD normalized these changes (Fig. 3A–D). PPARγ and PGC-1α are involved in the control of energy homeostasis and glucose metabolism (33,34). In addition, the level of expression of GLUT4 in adipocytes is implicated in the control of plasma glucose concentrations (35). Therefore, the TZD-mediated upregulation of PPARγ, PGC1-α and GLUT4 in adipocytes of R6/2 mice may contribute greatly to the improved lipogenesis and blood glucose homeostasis observed in these animals (Table 2, Fig. 2B). The observation that TZD treatment also reduced HTT aggregates, as assessed using a filter-retardation assay, in both subcutaneous and abdominal WATs was a somewhat surprising finding (Fig. 3E and F). Most importantly, PPARγ was recruited into HTT aggregates in adipocytes of R6/2 mice, which lowered the availability of PPARγ further. By reducing HTT aggregation, TZD treatment partially prevented the trapping of PPARγ in HTT aggregates, and thus led to the elevation of the levels of functional PPARγ in adipocytes.

To determine whether chronic TZD treatment affected the pathogenesis of HD in the brain, we investigated whether TZD reached the brain using liquid chromatography/tandem mass spectrometry (LC/MS/MS). As shown in Figure 4 and Table 4, TZD was detected in brain lysates harvested from R6/2 mice that were fed the TZD-supplemented diet, but not in animals that were fed the control diet. The TZD administration protocol employed in the present study allowed entry of the drug into the brain, where it exerted its beneficial effects. Similar to what was observed in adipocytes (Fig. 3), the level of the transcript of the downstream target gene of PPARγ, PGC-1α, was lower in the striatum of R6/2 mice compared with the striatum of WT mice (Fig. 5A). Chronic TZD treatment, which rescued the downregulation of PPARγ (Fig. 1A), also enhanced the striatal levels of the PGC-1α transcript significantly (Fig. 5A). This regulation of PGC1-α by mHTT was mediated by the suppression of PPARγ, as the expression of polyQ-expanded HTT in a striatal cell line also reduced the levels of the PGC-1α transcript; this effect was reversed by an agonist (Rosi) of PPARγ, in a GW9662-sensitive manner (Fig. 5B).

Stimulation of PPARγ promotes mitochondrial biogenesis and the remodeling of several peripheral tissues, via the induction of PGC-1α (33,36,37). Therefore, we evaluated whether mHTT compromised mitochondrial biogenesis via a PPARγ-dependent pathway in striatal cells expressing mHTT. The mitochondrial activity of ST14A cells was assessed using MitoGreen, which was used to determine mitochondrial mass (16,38). As shown in Figure 5C, the mitochondrial mass in Q_{158}-HTT-expressing cells was markedly lower than that observed in Q_{25}-HTT-expressing cells (Fig. 5C and D, and Supplementary Material, Fig. S2). Treatment with a PPARγ agonist (Rosi) enhanced the mitochondrial mass significantly, which was blocked by an antagonist of PPARγ (GW9662). This suggests that Rosi regulates the mitochondrial mass via a PPARγ-dependent pathway (Fig. 5C and D). The lower levels of PPARγ observed in striatal cells expressing mHTT may have resulted in insufficient expression of PGC1-α and subsequent poorer mitochondrial biogenesis. Consistent with the beneficial effects of TZD on mitochondrial biogenesis (31,39), our results suggest that the activation of PPARγ using agonists (TZD or Rosi) may rescue the lower density of mitochondria observed in HD via a PPARγ-dependent pathway.

Similar to what was observed in adipocytes (Fig. 3), we found that chronic TZD treatment reduced the number of HTT aggregates in the striatum of R6/2 mice (Fig. 6A and B). In addition, striatal PPARγ was also recruited into mHTT aggregates (Fig. 6C). TZD treatment may have enhanced the availability of functional PPARγ in the striatum, as assessed using western blot analysis (Fig. 6D), by reducing aggregate formation and, thus, preventing the sequestration of PPARγ in HTT aggregates.

Next, we investigated the potential mechanism through which TZD reduced the number of mHTT aggregates. For this, we assessed the involvement of the ubiquitin–proteasome system (UPS), as it mediates the degradation of misfolded proteins in an ATP-dependent manner and is markedly suppressed in HD (11,40–42). In addition, damaged mitochondria lead to inferior UPS activity, thus exacerbating aggregate formation in neurodegenerative diseases (40,43). We hypothesized that the deficiency in PGC1-α and the poor mitochondrial biogenesis observed in the presence of mHTT (Fig. 5) may have attributed to lower UPS activity. Using an anti-ubiquitin antibody and western blotting, we detected a marked increase in the amount of high-molecular-weight ubiquitin protein conjugates in the striatum of R6/2 mice (Fig. 7A), which suggests a defect in the UPS. Consistent with the hypothesis that improved energy homeostasis elevates UPS activity, chronic TZD treatment normalized the global ubiquitination profile,

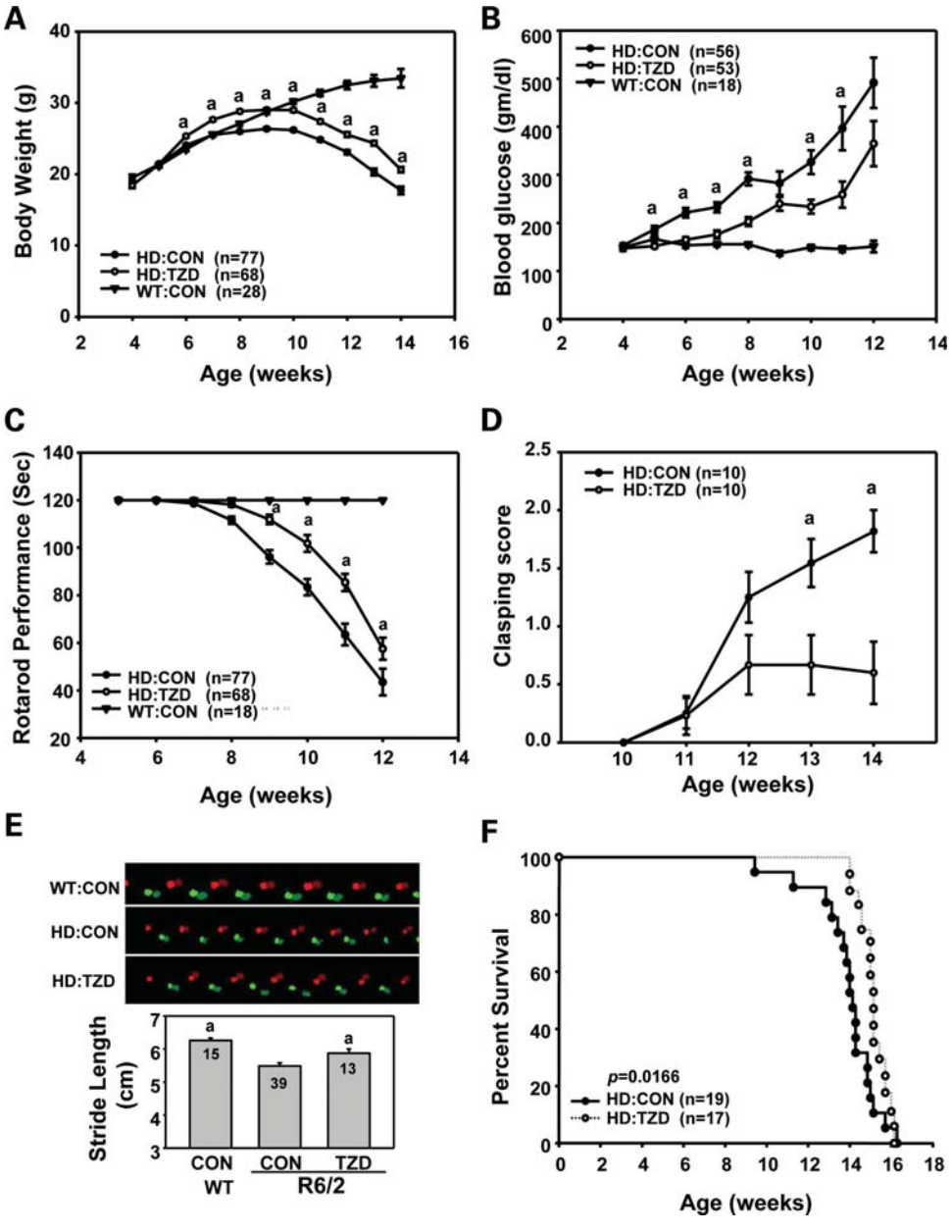

Figure 2. Chronic treatment with TZD produced beneficial effects in R6/2 mice. Mice were fed the control or 0.01% TZD-supplemented diet from the age of 4 weeks. Body weight (**A**), blood glucose (**B**), rotarod performance (**C**), clasping phenotype (**D**), gait status of mice at the age of 12 weeks (**E**) and survival (**F**) were assessed. Data are presented as the mean ± SEM. (A–E) [a]Specific comparison to HD mice fed control diet ($P < 0.05$; one-way ANOVA). (F) Specific comparison to HD mice fed the control diet ($P = 0.0166$; log-rank test).

at both the mid- and late-symptomatic stages of R6/2 mice (10.5 and 12 weeks of age, respectively). A more efficient UPS may degrade more mHTT and lead to a decrease in the formation of HTT aggregates. Filter-retardation assays revealed that the amount of HTT aggregates was lower in the striatum of R6/2 mice that were fed the TZD diet compared with animals that were fed the control diet (Fig. 6A). Mice that were fed the TZD diet also exhibited a reduced number of striatal cells containing HTT aggregates (Fig. 6B), which supports the notion that TZD treatment reduces the formation of HTT aggregates in the striatum of R6/2 mice. To validate this hypothesis, we expressed Q_{158}-HTT or Q_{25}-HTT in a striatal cell line and assessed UPS activity. As shown in Figure 7B, expression of Q_{158}-HTT decreased chymotrypsin-like activities, which was reversed by Rosi treatment. The effect of Rosi was blocked by GW9662, further demonstrating the involvement of PPARγ in the regulation of UPS activity.

To evaluate whether activation of PPARγ in the brain of R6/2 mice exerted a neuroprotective effect, we evaluated the expression levels of an important survival factor (Bcl-2) that is implicated in HD (44,45). This is of particular interest because Bcl-2 is a downstream target of PPARγ (46). We found that the level of the Bcl-2 protein was markedly

Table 2. Alterations in lipogenesis by chronic TZD treatment

Age (weeks)	10.5 weeks			12 weeks		
Genotype	WT	HD		WT	HD	
Diet	Control	Control	TZD	Control	Control	TZD
S/A fat ratio	55.3 ± 3.9	46.7 ± 5.7	68.1 ± 5.4[a]	39.5 ± 3.8	34.8 ± 5.8	88.2 ± 7.3[a]
BAT/A fat ratio	12.5 ± 1.2[a]	6.9 ± 0.9	16.8 ± 3.0[a]	9.6 ± 1.1[a]	5.9 ± 0.8	12.6 ± 2.7[a]

Animals ($n = 4 \sim 20$) were fed the control or TZD (0.01%)-supplemented diet from the age of 4 weeks. Values are expressed as the mean ± SEM.
S, subcutaneous white adipose tissue; A, abdominal white adipose tissue; BAT, brown adipose tissue.
[a]Specific comparison to HD mice fed the control diet ($P < 0.05$; one-way ANOVA).

Table 3. Metabolic parameters of R6/2 mice chronically fed a TZD diet

Age (weeks)	10.5 weeks			12 weeks		
Genotype	WT	HD		WT	HD	
Diet	Control	Control	TZD	Control	Control	TZD
Insulin (μg/l)	1.82 ± 0.38[a]	0.78 ± 0.12	0.56 ± 0.03	1.79 ± 0.52[a]	0.55 ± 0.03	0.51 ± 0.02
Triglycerides (mg/dl)	35.20 ± 2.26	28.86 ± 2.60	23.71 ± 2.81	34.42 ± 3.73	28.52 ± 1.86	22.03 ± 2.48
FFA (mmol/l)	2.26 ± 0.16	2.16 ± 0.08	1.68 ± 0.30	2.11 ± 0.17	1.62 ± 0.22	1.48 ± 0.26

Mice ($n = 4 \sim 6$) were fed the control or TZD (0.01%)-supplemented diet from the age of 4 weeks. Values are expressed as the mean ± SEM.
FFA, free fatty acid.
[a]Specific comparison between animals fed the control diet ($P < 0.05$; one-way ANOVA).

Table 4. Concentrations of TZD in the cortex of wild-type (WT) and R6/2 mice

Mice	Treatment	Rosiglitazone (ng/g)
WT	CON	n.d
R6/2	CON	n.d
R6/2	TZD	0.64 ± 0.14

Mice ($n = 6$) were fed the control or TZD (0.01%)-supplemented diet from the age of 4 weeks. Cortex lysates collected from 12-week-old animals were subjected to analyses. Values are expressed as the mean ± SEM.
CON, control diet; n.d., not detectable at the detection threshold of 1 pg/g brain lysate.

decreased in the striatum of R6/2 mice compared with the striatum of WT animals (Fig. 8A). Consistent with its beneficial effects, TZD upregulated the striatal Bcl-2 protein significantly (Fig. 8A). In addition, expression of Q_{158}-HTT in ST14A cells led to the downregulation of the Bcl-2 protein compared with cells expressing the control Q_{25}-HTT protein (Fig. 8B). Similar to what was observed in R6/2 mice, Rosi-mediated activation of PPARγ in ST14 cells upregulated the Bcl-2 protein, which was blocked by an antagonist (GW9662) of PPARγ.

To assess the neuroprotective effect of PPARγ activation in HD, we examined the effect of TZD on the levels of expression of the brain-derived neurotrophic factor (*BDNF*) in R6/2 mice. BDNF is critical for the survival of striatal neurons and is greatly suppressed during HD progression (21,47). qPCR analyses revealed that the levels of the *BDNF* transcript in the cortex and striatum of R6/2 mice were markedly reduced compared with those observed in WT mice (Fig. 9). Chronic TZD treatment enhanced the expression of *BDNF* transcripts in both the cortex and striatum of R6/2 mice, which suggests a general beneficial effect of TZD in the brain.

DISCUSSION

PPARγ is a ligand-activated nuclear receptor that has been implicated in diabetes and several major CNS diseases (48–51). In the present study, we determined the role of PPARγ in HD brain and peripheral tissues. Our findings led to the conclusion that deficient expression of PPARγ is an authentic manifestation that occurs in mice and patients with HD. We also analyzed the beneficial role of PPARγ agonists in the pathogenesis of HD. We found that the reduction of the levels of the PPARγ transcript (Fig. 1) and the recruitment of the PPARγ protein into mHTT aggregates (Fig. 6C) led to marked suppression of the activity of PPARγ by mHTT in multiple HD tissues, which may contribute to the energy deficiency observed in this devastating disease (Fig. 10). The poor PPARγ activity observed in HD led to the inevitable downregulation of many important downstream genes of PPARγ (e.g. *PGC-1α*, *Glut4* and *Bcl2*) in multiple tissues. For example, reduced PGC-1α expression was found in the striatum and adipocytes of HD (Figs 3 and 5), which may result in a decrease in the mitochondrial mass and in the production of ATP, thus subsequently altering a wide variety of ATP-dependent mechanisms, including the UPS (Fig. 7). Weakened UPS activity is expected to exacerbate aggregate formation and to worsen HD progression. In addition, lowered expression of GLUT4 (Fig. 3) in adipocytes is likely to be associated with the development of hyperglycemia (Fig. 2B) observed in HD (32). Downregulation of the neuroprotective gene *Bcl2*, as found in HD striatal cells (Fig. 8), may contribute to the neuronal dysfunction observed in HD brains (20). It is noteworthy that the levels of PPARγ in lymphocytes of HD patients were also lower than the levels detected in healthy volunteers (Fig. 1E), which suggests that downregulation of PPARγ may be a pathomechanism of HD. The clinical consequences of these findings are currently

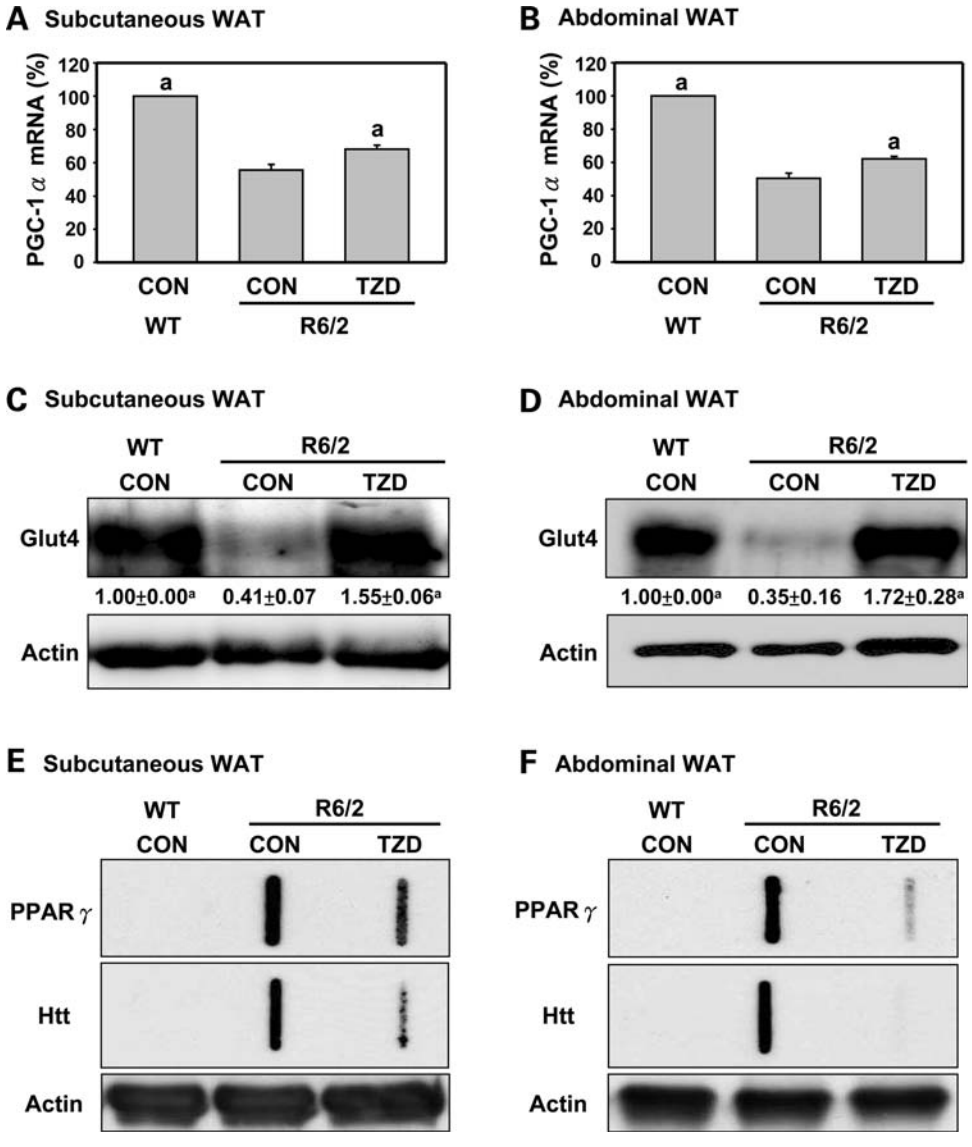

Figure 3. Chronic TZD treatment ameliorated recruitment of PPARγ into Htt aggregates, enhanced the reduced PGC-1α expression and elevated the reduced expression of Glut4 in WAT of R6/2 mice. Mice were fed the control or 0.01% TZD-supplemented diet from the age of 4 weeks. In the indicated 10.5-week-old mice, subcutaneous WAT (**A**) and abdominal WAT (**B**) were collected to determine the transcript level of PGC-1α using a quantitative RT–PCR technique. Expression levels of PGC-1α were normalized to that of HPRT. Subcutaneous WAT (**C**) and abdominal WAT (**D**) lysates (25 μg) were collected from the indicated 10.5-week-old mice, and subjected to a western blot analysis. Levels of the indicated protein were normalized with the corresponding internal control (actin), compared with those in wild-type mice, and then shown at the bottom of the corresponding lane. For the filter-retardation assays, subcutaneous WAT (**E**) and abdominal WAT (**F**) lysates (100 μg per slot) collected from the indicated 10.5-week-old mice were analyzed. The insoluble aggregates retained on the filters were detected using an anti-Htt or anti-PPARγ antibody. The level of actin in the WAT lysate was assessed using a western blot analysis and was used as the internal control. A representative image of three independent experiments is shown. Data are presented as the mean ± SEM from three independent experiments. [a]Specific comparison to HD mice fed the control diet ($P < 0.05$; one-way ANOVA).

unknown. Our study demonstrated that mHTT-mediated deficiency in PPARγ expression occurred in multiple organs and may contribute to the systematic dysregulation of energy homeostasis observed in HD.

Most importantly, activation of residual PPARγ using a well-characterized agonist (TZD) produced beneficial effects in both the CNS and peripheral HD tissues (Figs 2, 3 and 7–9), which suggests that, although PPARγ was downregulated in HD tissues, PPARγ represents a worthwhile drug target for this disease. Our findings are consistent with a recent study demonstrating that activation of PPARg by Rosi rescued the mitochondrial dysfunction caused by mHTT in a mouse striatal cell line (16). In the present study, we extended the demonstration of this rescue effect of PPARγ to the brain of HD mice. Chronic treatment with TZD significantly improved the reduced levels of two neuroprotective factors (Bcl-2 and BDNF) in the striatum of R6/2 mice and in mHTT-expressing ST14A cells (Figs 8 and 9). Together with the observation that TZD was detected in the brain of R6/2 mice that were fed a TZD-supplemented diet (Fig. 4C), our findings suggest that TZD exerts an important neuroprotective effect against the toxicity caused by mHTT *in vivo*.

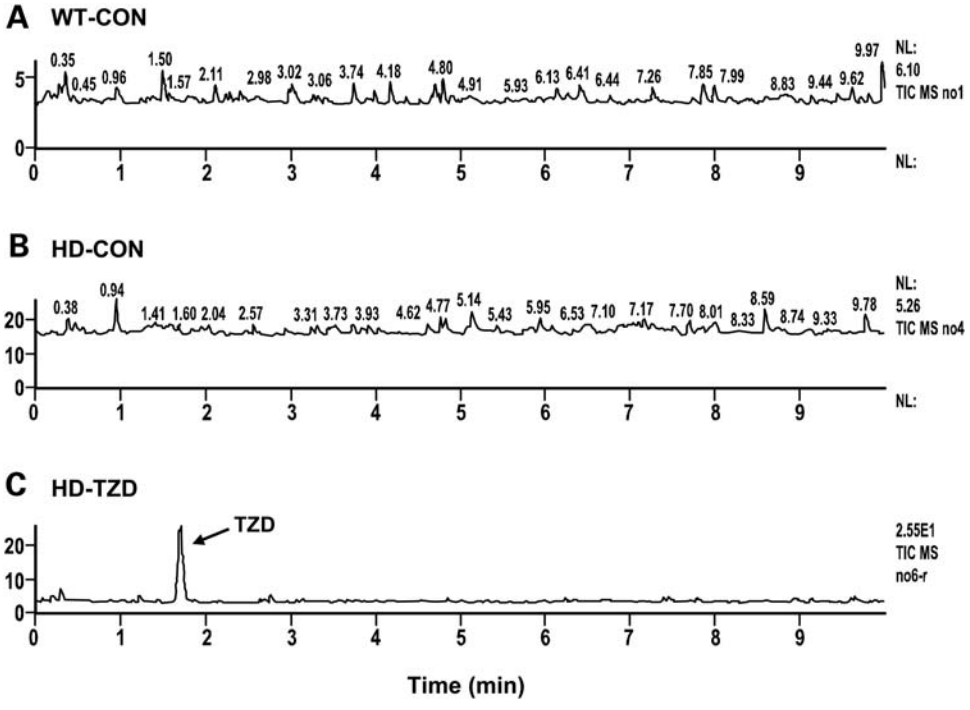

Figure 4. Liquid chromatographic tandem mass spectrometric chromatograms of cortical tissues of mice fed TZD. Mice were fed the control or 0.01% TZD-supplemented diet from the age of 4 weeks. Chromatograms of the cortical tissues harvested from the 12-week-old indicated mice were analyzed using the selected reaction monitoring mode. Representative chromatograms are shown.

The neuroprotective effect of PPARγ may be mediated by Bcl-2, which is a downstream target of PPARγ (46). A similar upregulation of Bcl-2 after PPARγ activation was reported in Neuro-2a and PC12 cells, in which PPARγ activation exerts a protective action against oxygen/glucose deprivation and amyloid β-mediated apoptosis, respectively (52,53).

Consistent with the protective effect of TZD in the brain, reduced UPS activity in the striatum of R6/2 mice was also enhanced by TZD (Fig. 7), which may contribute to the lower amount of neuronal intranuclear inclusions (Fig. 6) observed in the striatum of TZD-treated R6/2 mice compared with animals on the control diet (Fig. 6). Surprisingly, chronic TZD treatment did not produce a significant improvement in the brain atrophy of R6/2 mice. One major characteristic of HD mice is enlargement of ventricles accompanied by a progressive reduction in the brain weight (54). TZD did not ameliorate the increased ventricle-to-brain ratio of R6/2 mice, as assessed by *in vivo* 3D MRI imaging, or the reduced brain weight of R6/2 mice (Supplementary Material, Fig. S3). In addition, TZD did not enlarge the reduced size of neurons in the striatum of R6/2 mice, as assessed by Nissl staining (Supplementary Material, Fig. S4). Although chronic treatment with TZD normalized several prominent deficiencies in the brain of R6/2 mice and, thus, ameliorated the functions that were jeopardized by mHTT, these events may be insufficient to prevent neuronal atrophy effectively. It is important to note that food intake in HD mice is greatly reduced during disease progression. Thus, the amount of TZD intake via dietary supplement employed in the present study was gradually reduced in HD mice during disease progression, which may hinder the therapeutic effect of TZD. This may also contribute to the fact that the increase in survival time after chronic administration of the TZD dietary supplement was modest (Fig. 2F). Whether a more controlled administration of TZD (e.g. via osmotic minipumps), in conjunction with an additional means to enhance the PPARγ-mediated pathway (e.g. intrastriatal delivery of the *PPARγ* gene), would lead to more significant beneficial effects on striatal atrophy and life span warrants further investigation. Regardless of its apparent ineffectiveness in reducing brain atrophy, chronic TZD treatment clearly improved the motor dysfunction of R6/2 mice, as assessed using three different behavioral tests (rotarod performance, hind-limb clasping phenotype and gait analysis; Fig. 2C–E). This is not the first report on the failure of a beneficial agent for HD in preventing neuronal atrophy in HD mice (55,56). For example, an inhibitor of the Rho-associated kinase (Y-27632), which markedly improves rotarod performance and reduces the level of soluble mHTT protein in the brain of R6/2 mice, does not attenuate brain atrophy (55). A few other studies also indicate that improvements in motor function of HD mice are not always associated with prevention of striatal degeneration (56,57). Therefore, it cannot be excluded completely that neuronal dysfunction, which causes motor dysregulation, and neuronal atrophy are regulated by separate pathways (56). The protective functions of TZD in the brain of HD mice, regarding disease stage and neuronal activity/circuitry, are of great interest and require further investigation.

It is important to observe that chronic TZD treatment improved the body weight loss observed in the HD mice (Fig. 2A), because weight loss has long been recognized as an important symptom of HD patients (28,58). A higher

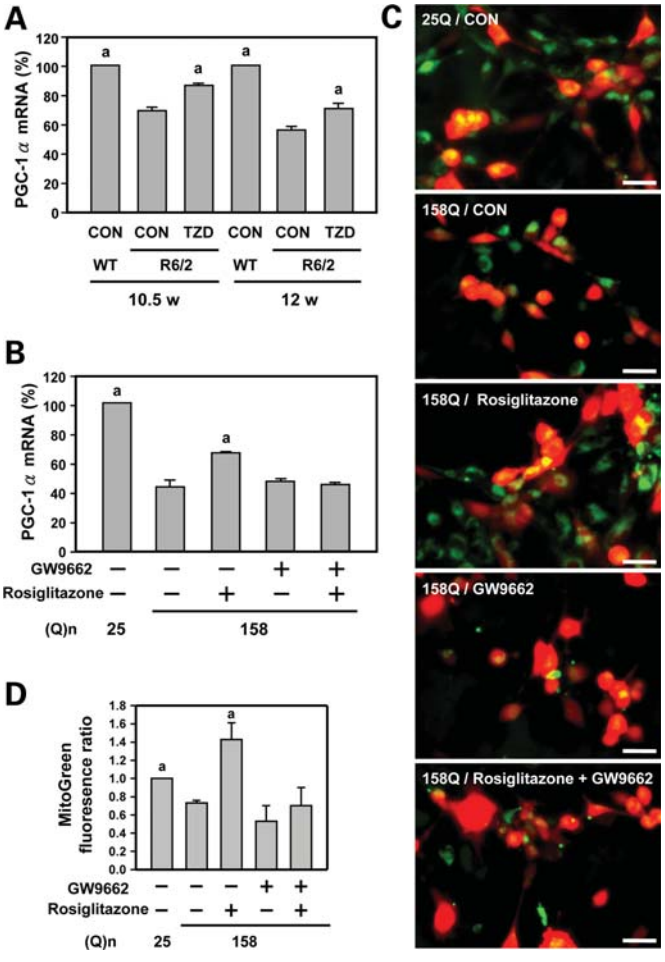

Figure 5. Activation of PPARγ enhanced the reduced PGC-1α and mitochondrial mass. Mice were fed the control or 0.01% thiazolidinedione (TZD)-supplemented diet from the age of 4 weeks. (**A**) From the indicated 10.5- and 12-week-old mice, striatal tissues were collected to determine the transcript level of PGC-1α using a quantitative RT–PCR technique. The expression levels of PGC-1α were normalized to that of GAPDH. Data are presented as the mean ± SEM from three independent experiments. The specific comparison with R6/2 mice fed the control diet is denoted 'a' ($P < 0.05$; one-way ANOVA). (**B**) ST14A cells were transfected with pcDNA3-(Htt-$(Q)_{25}$) or pcDNA3-(Htt-$(Q)_{158}$) for 24 h, and then treated with the indicated reagents (10 μM Rosi or 20 μM GW9662) for another 48 h. At the indicated conditions, cells were collected to determine the transcript level of PGC-1α using a quantitative RT–PCR technique. Expression levels of PGC-1α were normalized to that of GAPDH. Data are presented as the mean ± SEM from three independent experiments. [a]Specific comparison between the indicated group and that transfected with pcDNA3.1-$(Q)_{158}$-Htt with no treatment ($P < 0.05$; one-way ANOVA). (**C**) Cells were cotransfected with pcDNA3-(Htt-$(Q)_{25/158}$) and dsRFP DNA at a molar ratio of 4: 1 for 24 h, and then treated with the desired reagent(s) for another 48 h. Cells were collected to determine the mitochondrial mass using confocal microscopy. Expression of dsRFP is shown in red and the mitochondrial mass is shown in green. Scale bars, 50 μm. (**D**) Expression levels of the mitochondrial mass were normalized to that of dsRFP. Data are presented as the mean ± SEM from three independent experiments. [a]Specific comparison between the indicated group and that transfected with pcDNA3.1-$(Q)_{158}$-Htt with no treatment ($P < 0.05$; one-way ANOVA).

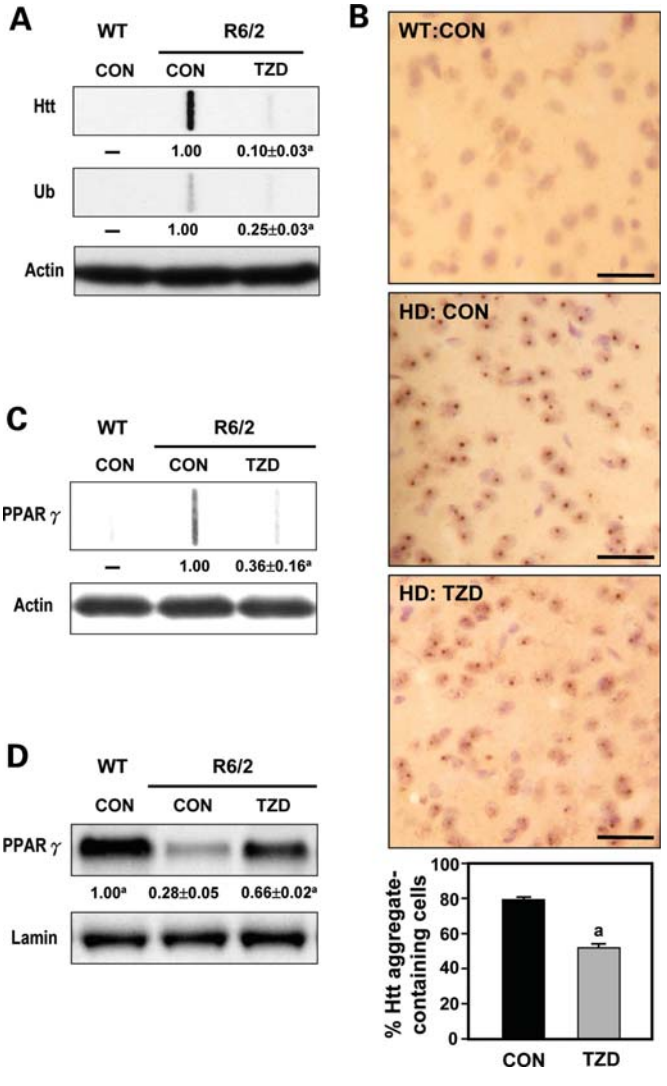

Figure 6. TZD reduced mHtt aggregate and ameliorated the recruitment of PPARγ by mHtt aggregates. Mice were fed the control or 0.01% TZD-supplemented diet from the age of 4 weeks. (**A**) Tissue lysates (50 μg) collected from 12-week-old mice were subjected to a filter-retardation assay. The insoluble Htt aggregates retained on the filter were detected using an anti-Htt or anti-ubiquitin antibody. (**B**) Representative images of the striatum of 12-week-old wild-type and R6/2 mice fed the indicated diet are shown. Htt aggregates were visualized with an antibody against ubiquitin. The percentages of striatal cells expressing NII were quantified (the right panel). [a]Specific comparison with R6/2 mice fed the control diet ($P < 0.05$; one-way ANOVA). Scale bars, 20 μm. (**C**) Tissue lysates (50 μg) collected from the indicated 12-week-old mice were subjected to a filter-retardation assay. Insoluble Htt aggregates retained on the filter were detected using an anti-PPARγ antibody, and normalized to actin. Data are presented as the mean ± SEM from three independent experiments. [a]Specific comparison with HD mice fed the control diet ($P < 0.05$; one-way ANOVA). (**D**) Nuclear extracts (100 μg) collected from the striatum of the indicated 12-week-old mice were analyzed for the expressions of PPARγ, and normalized to a nuclear marker (lamin). Data are presented as the mean ± SEM from three independent experiments.

body mass index is associated with a slower rate of disease progression (59). Part of the weight loss observed in HD may be associated with adipocyte dysfunction, as reported earlier (29,30) and in the present study (Table 2, Fig. 3). WAT is a major endocrine system that releases important factors and signaling molecules (such as adipokines, lipid moieties and fatty acids) to control body weight and energy homeostasis (60). The levels of adipokine hormones are altered in two different mouse models of HD (R6/2 mice and CAG140 knock-in mice) (29,30). In addition, expression

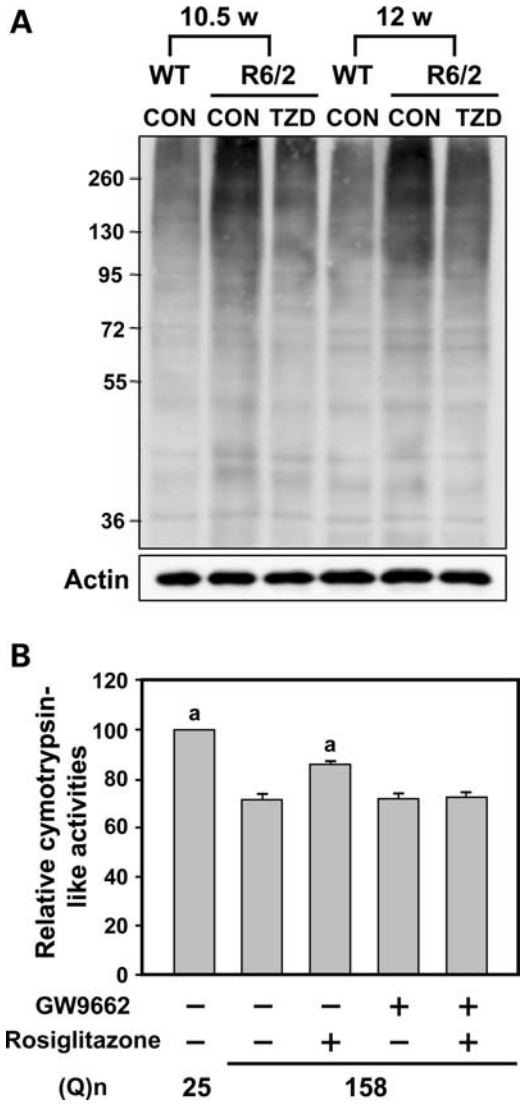

Figure 7. Activation of PPARγ enhanced the activities of the ubiquitin proteasome system compromised by mHtt. Mice were fed the control or 0.01% thiazolidinedione (TZD)-supplemented diet from the age of 4 weeks. (**A**) Striatal lysates (25 μg) collected from 10.5- and 12-week-old mice were subjected to Western blot analyses using an anti-ubiquitin antibody (upper panel) or an anti-actin antibody (lower panel). Representative pictures of three independent experiments are shown. (**B**) ST14A cells were transfected with pcDNA3-(Htt-$(Q)_{25}$) or pcDNA3-(Htt-$(Q)_{158}$) for 24 h, and then treated with the indicated reagents (10 μM Rosi or 20 μM GW9662) for another 48 h. At the indicated conditions, cells were collected to determine the chymotrypsin-like activity of proteasomes in the cellular lysates. Data are presented as the mean ± SEM from three independent experiments. [a]Specific comparison between the indicated group and that transfected with pcDNA3.1-$(Q)_{158}$-Htt with no treatment ($P < 0.05$; one-way ANOVA).

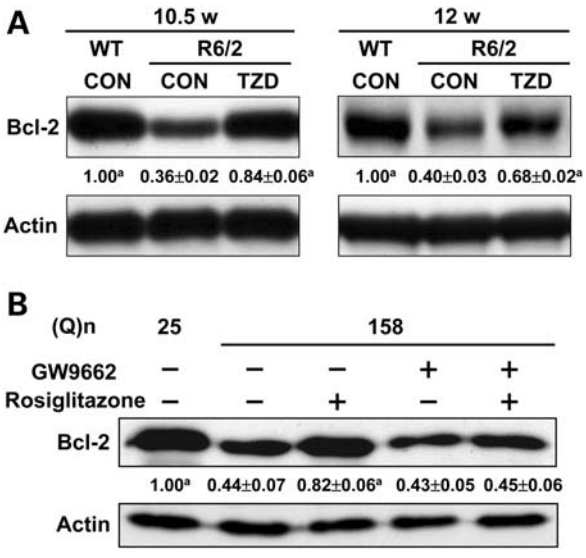

Figure 8. Activation of PPARγ enhanced the reduced Bcl-2 expression in striatal cells expressing mHtt. (**A**) Mice were fed the control or 0.01% TZD-supplemented diet from the age of 4 weeks. Striatal lysates (25 μg) collected from 10.5- and 12-week-old mice were subjected to Western blot analyses using an anti-Bcl-2 antibody (upper panel) or an anti-actin antibody (lower panel). Representative pictures of three independent experiments are shown. [a]Specific comparison to HD mice fed the control diet ($P < 0.05$; one-way ANOVA). (**B**) ST14A cells were transfected with pcDNA3-(Htt-$(Q)_{25}$) or pcDNA3-(Htt-$(Q)_{158}$) for 24 h, and then treated with the indicated reagents (10 μM Rosi or 20 μM GW9662) for another 48 h. Lysates (50 μg) harvested at the indicated conditions were subjected to a western blot analysis using an anti-Bcl-2 antibody (upper panel) or an anti-actin antibody (lower panel). Representative images of three independent experiments are shown. Data are presented as the mean ± SEM from three independent experiments. [a]Specific comparison between the indicated group and that transfected with pcDNA3.1-$(Q)_{158}$-Htt with no treatment ($P < 0.05$; one-way ANOVA).

of mHTT in 3T3-L1 adipocytes greatly reduces triglyceride storage (30). Thus, the expression of mHTT in adipocytes is believed to jeopardize the functions of adipokine hormones and to contribute to the weight loss that is characteristic of patients with HD. The action of mHTT in adipocytes may be mediated partly by its ability to suppress the expression and availability of PPARγ (Figs 1C and D, 3E and F). PPARγ is a transcription factor that is crucial for lipogenesis, adipocyte differentiation and body-fat distribution (34,51,61–63). Studies performed in mice with reduced levels of PPARγ showed that PPARγ is essential for the maintenance of the survival of mature adipocytes (64). Therefore, the low levels of PPARγ found in HD adipocytes (Fig. 1C and D) may cause a dysregulation in lipogenesis and adipocyte functions. Moreover, the detection of lower levels of GLUT4 in HD adipocytes compared with WT adipocytes (Fig. 3C and D) is of great interest, as *Glut4* is also a downstream target gene of PPARγ (32) and, when downregulated, is associated with hyperglycemia (65,66). Consistent with the concept that the impairment of PPARγ affects the functions of adipocytes critically, chronic treatment of R6/2 mice with TZD improved lipogenesis, elevated the reduced levels of GLUT4 and normalized hyperglycemia (Table 2, Figs 2B and 3). Our findings are consistent with an earlier study showing that Rosi enhances the levels of several key metabolic factors in subcutaneous and abdominal WATs (19). Interestingly, TZD treatment did not affect the reduced levels of insulin (Table 3). This was not surprising, as TZD improves insulin resistance without affecting its release (67). Our findings regarding adipocyte dysfunction are very important because, as suggested recently by Phan *et al.* (30), the treatment of dysregulated adipose tissues may improve the quality of life of HD patients. To the best of our knowledge, this is the first report

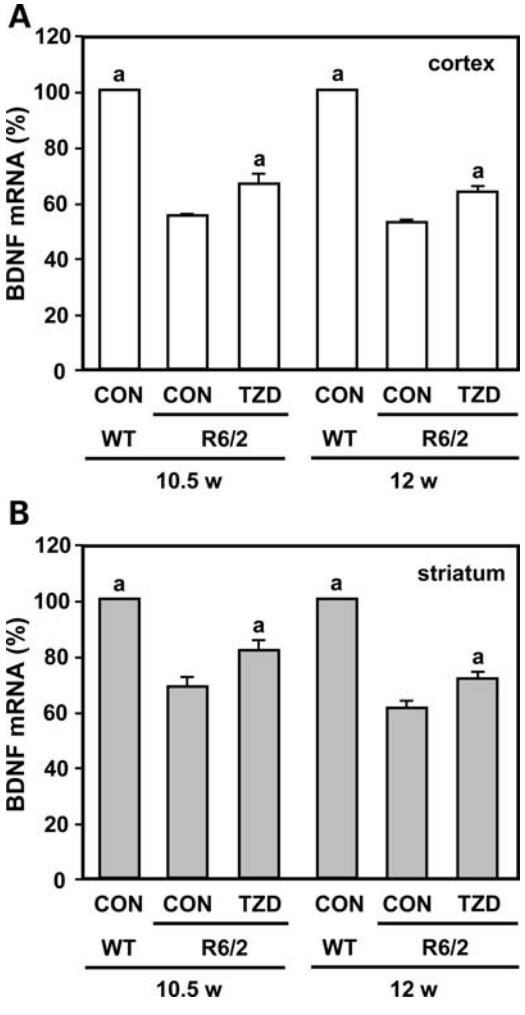

Figure 9. Chronic TZD treatment enhanced the reduced *BDNF* expression in the cortex and striatum of R6/2 mice. Mice were fed the control or 0.01% TZD-supplemented diet from the age of 4 weeks. At the indicated age, cortical (**A**) and striatal (**B**) tissues were collected to determine the transcript level of *BDNF* using a quantitative RT–PCR technique. The expression levels of *BDNF* were normalized to that of GAPDH. Data are presented as the mean ± SEM from three independent experiments. [a]Specific comparison with HD mice fed the control diet ($P < 0.05$; one-way ANOVA).

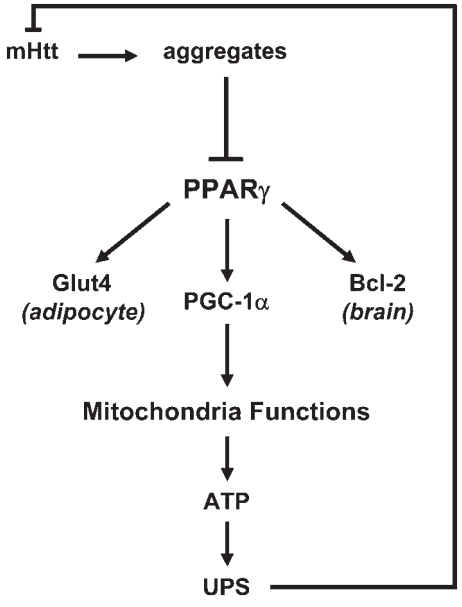

Figure 10. Schematic representation of the action of PPARγ in multiple tissues of HD. Expression of mHtt leads to formation of aggregates which inhibits the availability of PPARγ by reducing its transcript level and by recruiting its protein into aggregates. The poor PPARγ level and activity in multiple tissues of HD subsequently cause lower expressions of downstream target genes (e.g. PGC-1α in striatal cells and adipocytes, Glut4 in adipocytes, and Bcl2 in striatal cells) of PPARγ than those in wild-type mice. The deficiency in PGC-1α causes a reduced mitochondrial mass in HD, and thus compromises the functions of cellular machineries (e.g. the UPS) that require ATP. The weakened UPS activity further exacerbates aggregate formation and worsens the HD progression.

demonstrating that the deficient lipogenesis and weight loss observed in HD can be improved by activation of PPARγ.

Another critical downstream target of PPARγ is PGC-1α, which plays a critical role in mitochondrial biogenesis and energy homeostasis (33,68,69) and acts as a modifier of the age of onset of HD (70). Consistent with our observations that PPARγ was impaired in HD (Fig. 1), expression of PGC-1α is downregulated in several tissues of patients and mice with HD (namely, the brain, muscles and fatty tissues), as shown in several previous reports (30,68,69,71) and in the present study (Figs 3 and 5). This deficiency in PGC-1α is believed to cause mitochondrial dysfunction in the brains of patients and mice with HD (68). Genetic removal of PGC-1α enhances the progression of HD, as assessed by the monitoring of motor coordination and striatal neurodegeneration (68), which pinpoints the critical involvement of PGC-1α in HD. Our study also demonstrated that activation of PPARγ using its agonists enhanced the expression of PGC-1α in HD adipocytes, striatum and striatal cells (Figs 3 and 5). This upregulation of PGC-1α led to a subsequent increase in mitochondrial mass (Fig. 5C and D) and likely rescued a wide variety of machineries that suffered from energy deficiency in HD. In particular, the impairment of the energy-dependent UPS is critical, as it is responsible for the degradation of misfolded mutant proteins, which, if not cleaved efficiently, accumulate and form aberrant aggregates (41,72). Deficient mitochondrial activity impairs UPS activity in the brain of other degenerative diseases [Alzheimer's disease and Parkinson's disease (73,74)]. In HD, weakened UPS activity not only exacerbates aggregate formation but also damages the critical proofreading of misfolded proteins. By upregulating PGC-1α, chronic TZD treatment normalized the activity of the UPS, which was damaged by mHTT (Fig. 7), and delayed the progression of HD.

To date, there is no effective treatment for HD. None of the pharmacological interventions tested in eight clinical trials (1366 HD patients) were effective in delaying the progression of HD (75). As functional deficiencies were found in multiple tissues with HD, the simultaneous improvement of the PPARγ deficiency in both the CNS and peripheral tissues after TZD administration, as demonstrated in the present study, appears to be an effective therapeutic strategy. It is worth noting that an earlier study (76) reported that chronic treatment of R6/2 mice with Rosi (which is a form of TZD) at 3 mg/kg via daily intraperitoneal injection did not produce beneficial effects; those authors claimed that chronic treatment with

hypoglycemic agents does not alter the progression of HD. Nevertheless, no changes in blood glucose or body weight were found in those Rosi-treated R6/2 mice (76). Therefore, the dosage, treatment period and/or the protocol may not have been sufficient to sustain the effective activation of PPARγ-mediated pathways. In our study, TZD was administered as a dietary supplement, so that a constant low-level TZD was delivered to the animals. In addition, our daily dosage (~16.7 mg/kg) was ~4.5-fold higher than the one used in the study mentioned above (76). The reduced hyperglycemia, elevated body weight and increased expression of several downstream targets of PPARγ observed in R6/2 mice that were fed the TZD diet clearly demonstrate the effectiveness of the TZD treatment. Thus, the dosage and route of drug delivery seem to be critical for assessing whether TZD is a beneficial agent for HD. Moreover, TZD has been used for years to treat patients with type II diabetes; therefore, its possible side effects and toxicity have been explored extensively and are well understood. The potential novel application of TZD treatment to HD patients may require a much shorter period of trial compared with other new chemical entities. Given that multiple cellular machineries are damaged by mHTT in HD, strategies that combine TZD and other beneficial agents that affect aspects other than energy homeostasis have great therapeutic potential and deserve further investigation.

MATERIALS AND METHODS

Reagents

All reagents were purchased from Sigma (St. Louis, MO, USA) except where otherwise specified. Dulbecco's modified Eagle's medium (DMEM) and fetal bovine serum (FBS) were purchased from Invitrogen (Carlsbad, CA, USA). Rosiglitazone and GW9662 were from Cayman Chemicals (Ann Arbor, MI, USA).

Animals and drug administration

Male R6/2 mice and littermate controls were originally obtained from Jackson Laboratories (Bar Harbor, ME, USA), and maintained as previously described (20). TZD (Avandia) was purchased from Smith Klein Beecham (GSK, King of Prussia, PA, USA). Diets used in the present study were all prepared and purchased from LabDiet® (Richmond, VA, USA). Animal experiments were performed under protocols approved by the Academia Sinica Institutional Animal Care and Utilization Committee, Taipei, Taiwan.

Rotarod performance

Motor coordination was assessed using a rotarod apparatus (UGO BASILE, Comerio, Italy) at a constant speed (12 rpm) over the period of 2 min as described earlier (20).

Paw clasping

The clasping phenotype of R6/2 was evaluated as described previously (17), with slight modifications. Briefly, mice were suspended by the distal third of their tails for 30 s. Touch of the hind limbs were scored as follows: 0, no clasping; 1, clasping for 1–5 s and 2, clasping for longer than 5 s.

Gait analysis

The gait of WT and R6/2 mice was assessed using a CatWalk gait automatic analyzer (Noldus Information Technology, Leesburg, VA, USA), as described elsewhere (77). The position, timing and dimensions of each footfall were recorded by a video camera positioned underneath a glass plate. The stride distance and position of each paw from the midline were recorded and analyzed using ImageJ software (Research Services Branch of the National Institute of Mental Health, Bethesda, MD, USA) (78).

Measurements of blood glucose level

Blood glucose concentrations were measured using an ABBOTT Alcyon 300i analyzer (ABBOTT Labs, Abbott Park, IL, USA).

RNA isolation and qPCR

Total RNA was isolated and reverse-transcribed as detailed elsewhere (9). A real-time qPCR was performed using a TaqMan kit (PE Applied Biosystems, Foster City, CA, USA) on a TaqMan ABI 7500 Sequence Detection System (PE Applied Biosystems) using heat-activated TaqDNA polymerase (Amplitaq Gold; PE Applied Biosystems). The sequences of primers are listed in Supplementary Material, Table S2. Independent reverse-transcription PCRs were performed as described elsewhere (9). The relative transcript amount of the target gene, which was calculated using standard curves of serial RNA dilutions, was normalized to that of GAPDH or HPRT of the same RNA.

Western blot assays

Equal amounts of protein were separated by sodium dodecylsulfate–polyacrylamide gel electrophoresis (SDS–PAGE) using 10% polyacrylamide gels according to the method of Laemmli (79). The resolved proteins were electroblotted onto Immobilon polyvinylidene difluoride membranes (Millipore, Bedford, MA, USA) for the western blot analyses as described elsewhere (80). Primary antibodies of Bcl-2 (1:1000 dilution; Cell Signaling Technology, Danvers, MA, USA), PPARγ (1:1000; Cell Signaling Technology), Htt (1:500; Chemicon International, Temecula, CA, USA), Glut4 (1:3000; Abcam, Cambridge, MA, USA), ubiquitin (1:2000; DakoCytomation Denmark A/S, Glostrup, Denmark), actin (1:3000; Chemicon International) and lamin (1:2000; Santa Cruz Biotech, Santa Cruz, CA, USA) were utilized as recommended by the corresponding manufacturers.

Filter-retardation assay

The SDS-insoluble mutant Htt aggregates from the indicated tissues were retained on OE66 membrane filters (0.2 μm pore size, Whatman Schleicher and Schuell, Middlesex, UK) through a slot-blot manifold (Bio-Rad, Irvine, CA, USA),

and detected using the desired antibody (Htt, 1:1000; Chemicon International; ubiquitin, 1:2000; DakoCytomation Denmark A/S, Glostrup, Denmark; and PPARγ, 1:2000; Santa Cruz Biotechnology) as detailed elsewhere (10,81).

Immunohistochemistry and quantitation

Brain sections (20 μm) were used in the immunohistochemical analyses as described earlier (20). Cells harboring aggregates of mHtt were quantified in a blinded fashion. Single-antigen immunostaining was carried out using the avidin–biotin peroxidase complex method as previously described (82). In general, we used a 1:2000 dilution for the polyclonal anti-ubiquitin antiserum (DakoCytomation Denmark A/S). In total, four or five 12-week-old mice for each treatment were analyzed. Three different sections labeled with the anti-ubiquitin antiserum and counterstained with methyl green (Vector) from one tissue sample were quantified. The number of aggregate-containing cells was normalized with the number of total cells in each section and designated as the percent (%) of Htt aggregate-containing cells. At least 2800 cells from each brain section were quantified. Frozen serial sections were cut at 20 μm, stored in six-well plates and stained for Nissl substance by using cresyl violet as described earlier (77).

Cell culture

The striatal progenitor cell line (ST14A) was a generous gift from Dr E. Cattaneo (University of Milano, Milano, Italy) and was maintained in an incubation chamber gassed with 10% CO_2 and 90% air at 33°C as previously described (83). The day before transfection, cells were seeded onto a 35 mm dish at a density of 1×10^5 cells per well. Cells were transfected with pcDNA3-(Htt-$(Q)_{25}$) or pcDNA3-(Htt-$(Q)_{158}$) using Lipofectamine 2000 (LF2000, Invitrogen) for 24 h, and then treated with the desired reagent(s) for another 48 h.

Mitochondrial mass

The fluorescent probe Mitotracker GreenTM dye (MitoGreen, Invitrogen) binds to mitochondrial membrane lipids regardless of the mitochondrial membrane potential or oxidant status (84). To determine the levels of mitochondria, cells were loaded with 0.2 mM/ml Mitotracker GreenTM dye medium for 30 min at 37°C. Fluorescence measurements were made with excitation at 490 nm and emission at 516 nm using an Axiovert 200 live cell observation system (Carl Ziess, Göttingen G). Amounts were determined by comparing the means of the fluorescent signal.

Sample preparation and LC/MS/MS method

Cortical tissues (20–40 mg) were dissected and weighed. Samples were transferred to a high-clarity polypropylene tube in an ice bath containing 400 μl of methanol and 4 μl of formic acid. The tissue in the tube was homogenized using a pro 200 hand-held homogenizer with a 7 mm sawtooth bottom generator (PRO Scientific, Oxford, CT, USA). The homogenate was then centrifuged at 14 000 rpm for 10 min at 0°C. The supernatant was further diluted with 10 mM ammonium acetate buffer (pH 8.0) to 2 ml. The diluted sample (0.5 ml) was loaded on an Oasis HLB μElution plate (Waters, Miford, MA, USA), which was preconditioned with 0.5 ml of methanol, 0.5 ml of water and 0.5 ml of 10 mM ammonium acetate buffer (pH 8.0). After sample loading, the cartridge was washed with 0.5 ml of water and eluted with 0.1 ml of acetonitrile. The eluent was collected for the LC/MS/MS analysis. Briefly, the LC system used was a Surveyor MS pump plus HPLC coupled with a Surveyor autosampler plus. Chromatographic separation was achieved using an XBridge C_{18} column (2.1 × 150 mm with a 5 μm particle size) (Waters). The LC operating conditions were isocratic separation, which was previously described (25). Solvents were degassed online, and the flow rate was 0.3 ml/min. The autosampler was set to 0°C and the column temperature was maintained at 25°C. The sample injection volume was 5 μl. The MS analysis was carried out on a TSQ Quantum Ultra EMR triple quadrupole MS (ThermoFisher, San Jose, CA, USA). Samples were analyzed by atmospheric pressure chemical ionization with positive polarity, using highly selected reaction monitoring (H-SRM) for quantification. The MS/MS conditions were as follows: the SRM transition was m/z $358 > 135$; and argon gas was used as the collisional gas at 1.5 mTorr pressure and 25 eV energy. Xcalibur vers. 2.0 software was used for data acquisition and processing.

Luciferase assays

Luciferase activities of Htt-expressing ST14A cells were determined using the Dual-Luciferase Reporter Assay System (Promega) as described elsewhere (9). The protein concentrations of lysates were determined by the Bradford analysis, and the luciferase activities were normalized to the amount of proteins in the lysate. At least three independent transfections were performed for each experiment.

Proteasome activity assay

Proteasome activities of Htt-expressing ST14A cells were determined using a specific proteasome substrate [succinyl-Leu-Leu-Val-Tyr-7-amino-4-methyl coumarin (AMC) (Sigma-Aldrich)] as described elsewhere (11). Total lysate (10 μg) was prepared by resuspending cells, and the fluorescence of the released AMC was detected using a Fluorescence Microplate Reader System (Device, Sunnyvale, CA, USA) at 380 nm excitation and 460 nm emission wavelengths. At least three independent transfections were performed for each experiment.

Subjects

Seventeen genetically confirmed HD patients and 18 age- and gender-matched healthy controls with no neurological disease were recruited (Table 1). The Unified Huntington's Disease Rating Scale (UHDRS) (85) was recorded for each patient.

PPARγ of leukocytes of study subjects

Seventeen patients with HD (6 women and 11 men, 50.41 ± 3.12 years old, with 44.18 ± 1.49 CAG repeats) and 18 age- and gender-matched controls with no known neurological disease (7 women and 11 men, 51.00 ± 2.94 years old) were

studied. Diagnosis of HD was established by a neurological examination and genetic assessment of CAG expansion in the Htt gene. A leukocyte sample was drawn from the vein of each overnight-fasting subject after obtaining informed consent. The protocol was in compliance with guidelines of the Institutional Review Boards of Chang Gung Memorial Hospital, Taipei Veterans General Hospital, and Academia Sinica (Taipei, Taiwan). Leukocyte samples were collected from 18 control subjects (CON) and 17 HD patients (HD) for PPARγ expression measurement by a quantitative RT–PCR technique. The expression levels of PPARγ were normalized to that of GAPDH. Relative gene expressions were calculated using the $2^{\Delta C_T}$ method, $\Delta C_T = C_T(\text{GAPDH}) - C_T(\text{PPAR}\gamma)$, in which C_T indicates the cycle threshold (the fractional cycle number where the fluorescent signal reaches the detection threshold).

SUPPLEMENTARY MATERIAL

Supplementary Material is available at *HMG* online.

ACKNOWLEDGEMENTS

We thank Dr Pei Chen and Ms Shu-Yi, Lin for consultation on statistical analyses, and Dr Pauline Yen and Mr Dan Chamberlin for reading and editing the manuscript.

Conflict of Interest statement. None declared.

FUNDING

This work was supported by grants from the National Science Council (NSC96-2321-B-001-015, NSC 97-2321-B-001-012 and NSC97-2321-B-001-030 to Y.C., and NSC96-2321-B-320-003 and NSC97-2320-B-034-001-MY2 to M.C.C.) and Academia Sinica (AS-94-TP-B17 and AS-97-TP-B02 to Y.C.), Taiwan.

REFERENCES

1. Huntington's Disease Collaborative Research Group. (1993) A novel gene containing a trinucleotide repeat that is expanded and unstable on Huntington's disease chromosomes. The Huntington's Disease Collaborative Research Group. *Cell*, **72**, 971–983.
2. Vonsattel, J.P., Myers, R.H., Stevens, T.J., Ferrante, R.J., Bird, E.D. and Richardson, E.P. Jr (1985) Neuropathological classification of Huntington's disease. *J. Neuropathol. Exp. Neurol.*, **44**, 559–577.
3. Reddy, P.H., Williams, M. and Tagle, D.A. (1999) Recent advances in understanding the pathogenesis of Huntington's disease. *Trends Neurosci.*, **22**, 248–255.
4. Waelter, S., Boeddrich, A., Lurz, R., Scherzinger, E., Lueder, G., Lehrach, H. and Wanker, E.E. (2001) Accumulation of mutant huntingtin fragments in aggresome-like inclusion bodies as a result of insufficient protein degradation. *Mol. Biol. Cell*, **12**, 1393–1407.
5. Jana, N.R., Tanaka, M., Wang, G.-H. and Nukina, N. (2000) Polyglutamine length-dependent interaction of Hsp40 and Hsp70 family chaperones with truncated N-terminal huntingtin: their role in suppression of aggregation and cellular toxicity. *Hum. Mol. Genet.*, **9**, 2009–2018.
6. Suhr, S.T., Senut, M.C., Whitelegge, J.P., Faull, K.F., Cuizon, D.B. and Gage, F.H. (2001) Identities of sequestered proteins in aggregates from cells with induced polyglutamine expression. *J. Cell Biol.*, **153**, 283–294.
7. Steffan, J.S., Kazantsev, A., Spasic-Boskovic, O., Greenwald, M., Zhu, Y.Z., Gohler, H., Wanker, E.E., Bates, G.P., Housman, D.E. and Thompson, L.M. (2000) The Huntington's disease protein interacts with p53 and CREB-binding protein and represses transcription. *Proc. Natl Acad. Sci. USA*, **97**, 6763–6768.
8. Dunah, A.W., Jeong, H., Griffin, A., Kim, Y.M., Standaert, D.G., Hersch, S.M., Mouradian, M.M., Young, A.B., Tanese, N. and Krainc, D. (2002) Sp1 and TAFII130 transcriptional activity disrupted in early Huntington's disease. *Science*, **296**, 2238–2243.
9. Chiang, M.C., Lee, Y.C., Huang, C.L. and Chern, Y. (2005) cAMP-response element-binding protein contributes to suppression of the A2A adenosine receptor promoter by mutant Huntingtin with expanded polyglutamine residues. *J. Biol. Chem.*, **280**, 14331–14340.
10. Chiang, M.C., Chen, H.M., Lee, Y.H., Chang, H.H., Wu, Y.C., Soong, B.W., Chen, C.M., Wu, Y.R., Liu, C.S., Niu, D.M. *et al.* (2007) Dysregulation of C/EBPalpha by mutant Huntingtin causes the urea cycle deficiency in Huntington's disease. *Hum. Mol. Genet.*, **16**, 483–498.
11. Chiang, M.C., Chen, H.M., Lai, H.L., Chen, H.W., Chou, S.Y., Chen, C.M., Tsai, F.J. and Chern, Y. (2009) The A2A adenosine receptor rescues the urea cycle deficiency of Huntington's disease by enhancing the activity of the ubiquitin–proteasome system. *Hum. Mol. Genet.*, **18**, 2929–2942.
12. Podolsky, S., Leopold, N.A. and Sax, D.S. (1972) Increased frequency of diabetes mellitus in patients with Huntington's chorea. *Lancet*, **1**, 1356–1358.
13. Underwood, B.R., Broadhurst, D., Dunn, W.B., Ellis, D.I., Michell, A.W., Vacher, C., Mosedale, D.E., Kell, D.B., Barker, R.A., Grainger, D.J. *et al.* (2006) Huntington disease patients and transgenic mice have similar pro-catabolic serum metabolite profiles. *Brain*, **129**, 877–886.
14. Valenza, M., Carroll, J.B., Leoni, V., Bertram, L.N., Bjorkhem, I., Singaraja, R.R., Di Donato, S., Lutjohann, D., Hayden, M.R. and Cattaneo, E. (2007) Cholesterol biosynthesis pathway is disturbed in YAC128 mice and is modulated by huntingtin mutation. *Hum. Mol. Genet.*, **16**, 2187–2198.
15. Rosen, E.D., Hsu, C.H., Wang, X., Sakai, S., Freeman, M.W., Gonzalez, F.J. and Spiegelman, B.M. (2002) C/EBPalpha induces adipogenesis through PPARgamma: a unified pathway. *Genes Dev.*, **16**, 22–26.
16. Quintanilla, R.A., Jin, Y.N., Fuenzalida, K., Bronfman, M. and Johnson, G.V. (2008) Rosiglitazone treatment prevents mitochondrial dysfunction in mutant huntingtin-expressing cells: possible role of peroxisome proliferator-activated receptor-gamma (PPARgamma) in the pathogenesis of Huntington disease. *J. Biol. Chem.*, **283**, 25628–25637.
17. Mangiarini, L., Sathasivam, K., Seller, M., Cozens, B., Harper, A., Hetherington, C., Lawton, M., Trottier, Y., Lehrach, H., Davies, S.W. *et al.* (1996) Exon 1 of the HD gene with an expanded CAG repeat is sufficient to cause a progressive neurological phenotype in transgenic mice. *Cell*, **87**, 493–506.
18. Fajas, L., Auboeuf, D., Raspe, E., Schoonjans, K., Lefebvre, A.M., Saladin, R., Najib, J., Laville, M., Fruchart, J.C., Deeb, S. *et al.* (1997) The organization, promoter analysis, and expression of the human PPARgamma gene. *J. Biol. Chem.*, **272**, 18779–18789.
19. Walker, G.E., Marzullo, P., Verti, B., Guzzaloni, G., Maestrini, S., Zurleni, F., Liuzzi, A. and Di Blasio, A.M. (2008) Subcutaneous abdominal adipose tissue subcompartments: potential role in rosiglitazone effects. *Obesity (Silver Spring)*, **16**, 1983–1991.
20. Chou, S.Y., Lee, Y.C., Chen, H.M., Chiang, M.C., Lai, H.L., Chang, H.H., Wu, Y.C., Sun, C.N., Chien, C.L., Lin, Y.S. *et al.* (2005) CGS21680 attenuates symptoms of Huntington's disease in a transgenic mouse model. *J. Neurochem.*, **93**, 310–320.
21. Duan, W., Guo, Z., Jiang, H., Ware, M., Li, X.J. and Mattson, M.P. (2003) Dietary restriction normalizes glucose metabolism and BDNF levels, slows disease progression, and increases survival in huntingtin mutant mice. *Proc. Natl Acad. Sci. USA*, **100**, 2911–2916.
22. Lalic, N.M., Maric, J., Svetel, M., Jotic, A., Stefanova, E., Lalic, K., Dragasevic, N., Milicic, T., Lukic, L. and Kostic, V.S. (2008) Glucose homeostasis in Huntington disease: abnormalities in insulin sensitivity and early-phase insulin secretion. *Arch. Neurol.*, **65**, 476–480.
23. Bhatia, V. and Viswanathan, P. (2006) Insulin resistance and PPAR insulin sensitizers. *Curr. Opin. Investig. Drugs*, **7**, 891–897.
24. Hurlbert, M.S., Zhou, W., Wasmeier, C., Kaddis, F.G., Hutton, J.C. and Freed, C.R. (1999) Mice transgenic for an expanded CAG repeat in the Huntington's disease gene develop diabetes. *Diabetes*, **48**, 649–651.
25. Chou, C.C., Lee, M.R., Cheng, F.C. and Yang, D.Y. (2005) Solid-phase extraction coupled with liquid chromatography-tandem mass spectrometry

for determination of trace rosiglitazone in urine. *J. Chromatogr. A*, **1097**, 74–83.
26. van Dellen, A., Blakemore, C., Deacon, R., York, D. and Hannan, A.J. (2000) Delaying the onset of Huntington's in mice. *Nature*, **404**, 721–722.
27. Tsai, Y.S., Tsai, P.J., Jiang, M.J., Chou, T.Y., Pendse, A., Kim, H.S. and Maeda, N. (2009) Decreased PPAR gamma expression compromises perigonadal-specific fat deposition and insulin sensitivity. *Mol. Endocrinol.*, **23**, 1787–1798.
28. Aziz, N.A., van der Burg, J.M., Landwehrmeyer, G.B., Brundin, P., Stijnen, T. and Roos, R.A. (2008) Weight loss in Huntington disease increases with higher CAG repeat number. *Neurology*, **71**, 1506–1513.
29. Fain, J.N., Del Mar, N.A., Meade, C.A., Reiner, A. and Goldowitz, D. (2001) Abnormalities in the functioning of adipocytes from R6/2 mice that are transgenic for the Huntington's disease mutation. *Hum. Mol. Genet.*, **10**, 145–152.
30. Phan, J., Hickey, M.A., Zhang, P., Chesselet, M.F. and Reue, K. (2009) Adipose tissue dysfunction tracks disease progression in two Huntington's disease mouse models. *Hum. Mol. Genet.*, **18**, 1006–1016.
31. Hondares, E., Mora, O., Yubero, P., Rodriguez de la Concepcion, M., Iglesias, R., Giralt, M. and Villarroya, F. (2006) Thiazolidinediones and rexinoids induce peroxisome proliferator-activated receptor-coactivator (PGC)-1alpha gene transcription: an autoregulatory loop controls PGC-1alpha expression in adipocytes via peroxisome proliferator-activated receptor-gamma coactivation. *Endocrinology*, **147**, 2829–2838.
32. Armoni, M., Kritz, N., Harel, C., Bar-Yoseph, F., Chen, H., Quon, M.J. and Karnieli, E. (2003) Peroxisome proliferator-activated receptor-gamma represses GLUT4 promoter activity in primary adipocytes, and rosiglitazone alleviates this effect. *J. Biol. Chem.*, **278**, 30614–30623.
33. Puigserver, P. and Spiegelman, B.M. (2003) Peroxisome proliferator-activated receptor-gamma coactivator 1 alpha (PGC-1 alpha): transcriptional coactivator and metabolic regulator. *Endocr. Rev.*, **24**, 78–90.
34. Lehrke, M. and Lazar, M.A. (2005) The many faces of PPARgamma. *Cell*, **123**, 993–999.
35. Liu, M.L., Gibbs, E.M., McCoid, S.C., Milici, A.J., Stukenbrok, H.A., McPherson, R.K., Treadway, J.L. and Pessin, J.E. (1993) Transgenic mice expressing the human GLUT4/muscle-fat facilitative glucose transporter protein exhibit efficient glycemic control. *Proc. Natl Acad. Sci. USA*, **90**, 11346–11350.
36. Wu, Z., Puigserver, P., Andersson, U., Zhang, C., Adelmant, G., Mootha, V., Troy, A., Cinti, S., Lowell, B., Scarpulla, R.C. *et al.* (1999) Mechanisms controlling mitochondrial biogenesis and respiration through the thermogenic coactivator PGC-1. *Cell*, **98**, 115–124.
37. Pagel-Langenickel, I., Bao, J., Joseph, J.J., Schwartz, D.R., Mantell, B.S., Xu, X., Raghavachari, N. and Sack, M.N. (2008) PGC-1alpha integrates insulin signaling, mitochondrial regulation, and bioenergetic function in skeletal muscle. *J. Biol. Chem.*, **283**, 22464–22472.
38. Wilson-Fritch, L., Burkart, A., Bell, G., Mendelson, K., Leszyk, J., Nicoloro, S., Czech, M. and Corvera, S. (2003) Mitochondrial biogenesis and remodeling during adipogenesis and in response to the insulin sensitizer rosiglitazone. *Mol. Cell. Biol.*, **23**, 1085–1094.
39. Guan, H.P., Ishizuka, T., Chui, P.C., Lehrke, M. and Lazar, M.A. (2005) Corepressors selectively control the transcriptional activity of PPARgamma in adipocytes. *Genes Dev.*, **19**, 453–461.
40. Ross, C.A. and Pickart, C.M. (2004) The ubiquitin–proteasome pathway in Parkinson's disease and other neurodegenerative diseases. *Trends Cell Biol.*, **14**, 703–711.
41. Nandi, D., Tahiliani, P., Kumar, A. and Chandu, D. (2006) The ubiquitin–proteasome system. *J. Biosci.*, **31**, 137–155.
42. Bennett, E.J., Shaler, T.A., Woodman, B., Ryu, K.Y., Zaitseva, T.S., Becker, C.H., Bates, G.P., Schulman, H. and Kopito, R.R. (2007) Global changes to the ubiquitin system in Huntington's disease. *Nature*, **448**, 704–708.
43. Domingues, A.F., Arduino, D.M., Esteves, A.R., Swerdlow, R.H., Oliveira, C.R. and Cardoso, S.M. (2008) Mitochondria and ubiquitin–proteasomal system interplay: relevance to Parkinson's disease. *Free Radic. Biol. Med.*, **45**, 820–825.
44. Zhang, Y., Ona, V.O., Li, M., Drozda, M., Dubois-Dauphin, M., Przedborski, S., Ferrante, R.J. and Friedlander, R.M. (2003) Sequential activation of individual caspases, and of alterations in Bcl-2 proapoptotic signals in a mouse model of Huntington's disease. *J. Neurochem.*, **87**, 1184–1192.
45. Duan, W., Peng, Q., Masuda, N., Ford, E., Tryggestad, E., Ladenheim, B., Zhao, M., Cadet, J.L., Wong, J. and Ross, C.A. (2008) Sertraline slows disease progression and increases neurogenesis in N171-82Q mouse model of Huntington's disease. *Neurobiol. Dis.*, **30**, 312–322.
46. Butts, B.D., Tran, N.L. and Briehl, M.M. (2004) Identification of a functional peroxisome proliferator activated receptor response element in the 3′ untranslated region of the human bcl-2 gene. *Int. J. Oncol.*, **24**, 1305–1310.
47. Zuccato, C., Ciammola, A., Rigamonti, D., Leavitt, B.R., Goffredo, D., Conti, L., MacDonald, M.E., Friedlander, R.M., Silani, V., Hayden, M.R. *et al.* (2001) Loss of huntingtin-mediated BDNF gene transcription in Huntington's disease. *Science*, **293**, 493–498.
48. Sundararajan, S., Jiang, Q., Heneka, M. and Landreth, G. (2006) PPARgamma as a therapeutic target in central nervous system diseases. *Neurochem. Int.*, **49**, 136–144.
49. Landreth, G. (2006) PPARgamma agonists as new therapeutic agents for the treatment of Alzheimer's disease. *Exp. Neurol.*, **199**, 245–248.
50. Bordet, R., Ouk, T., Petrault, O., Gele, P., Gautier, S., Laprais, M., Deplanque, D., Duriez, P., Staels, B., Fruchart, J.C. *et al.* (2006) PPAR: a new pharmacological target for neuroprotection in stroke and neurodegenerative diseases. *Biochem. Soc. Trans.*, **34**, 1341–1346.
51. Lazar, M.A. (2005) PPAR gamma, 10 years later. *Biochimie*, **87**, 9–13.
52. Fuenzalida, K., Quintanilla, R., Ramos, P., Piderit, D., Fuentealba, R.A., Martinez, G., Inestrosa, N.C. and Bronfman, M. (2007) Peroxisome proliferator-activated receptor gamma up-regulates the Bcl-2 anti-apoptotic protein in neurons and induces mitochondrial stabilization and protection against oxidative stress and apoptosis. *J. Biol. Chem.*, **282**, 37006–37015.
53. Wu, J.S., Lin, T.N. and Wu, K.K. (2009) Rosiglitazone and PPAR-gamma overexpression protect mitochondrial membrane potential and prevent apoptosis by upregulating anti-apoptotic Bcl-2 family proteins. *J. Cell. Physiol.*, **220**, 58–71.
54. Ferrante, R.J., Andreassen, O.A., Jenkins, B.G., Dedeoglu, A., Kuemmerle, S., Kubilus, J.K., Kaddurah-Daouk, R., Hersch, S.M. and Beal, M.F. (2000) Neuroprotective effects of creatine in a transgenic mouse model of Huntington's disease. *J. Neurosci.*, **20**, 4389–4397.
55. Li, M., Huang, Y., Ma, A.A., Lin, E. and Diamond, M.I. (2009) Y-27632 improves rotarod performance and reduces huntingtin levels in R6/2 mice. *Neurobiol. Dis.*, **36**, 413–420.
56. Van Raamsdonk, J.M., Pearson, J., Rogers, D.A., Lu, G., Barakauskas, V.E., Barr, A.M., Honer, W.G., Hayden, M.R. and Leavitt, B.R. (2005) Ethyl-EPA treatment improves motor dysfunction, but not neurodegeneration in the YAC128 mouse model of Huntington disease. *Exp. Neurol.*, **196**, 266–272.
57. Van Raamsdonk, J.M., Pearson, J., Bailey, C.D., Rogers, D.A., Johnson, G.V., Hayden, M.R. and Leavitt, B.R. (2005) Cystamine treatment is neuroprotective in the YAC128 mouse model of Huntington disease. *J. Neurochem.*, **95**, 210–220.
58. Nance, M.A. and Sanders, G. (1996) Characteristics of individuals with Huntington disease in long-term care. *Mov. Disord.*, **11**, 542–548.
59. Myers, R.H., Sax, D.S., Koroshetz, W.J., Mastromauro, C., Cupples, L.A., Kiely, D.K., Pettengill, F.K. and Bird, E.D. (1991) Factors associated with slow progression in Huntington's disease. *Arch. Neurol.*, **48**, 800–804.
60. Trayhurn, P., Bing, C. and Wood, I.S. (2006) Adipose tissue and adipokines—energy regulation from the human perspective. *J. Nutr.*, **136**, 1935S–1939S.
61. Rosen, E.D., Walkey, C.J., Puigserver, P. and Spiegelman, B.M. (2000) Transcriptional regulation of adipogenesis. *Genes Dev.*, **14**, 1293–1307.
62. Spiegelman, B.M. (1998) PPAR-gamma: adipogenic regulator and thiazolidinedione receptor. *Diabetes*, **47**, 507–514.
63. Tsai, Y.S. and Maeda, N. (2005) PPARgamma: a critical determinant of body fat distribution in humans and mice. *Trends Cardiovasc. Med.*, **15**, 81–85.
64. He, W., Barak, Y., Hevener, A., Olson, P., Liao, D., Le, J., Nelson, M., Ong, E., Olefsky, J.M. and Evans, R.M. (2003) Adipose-specific peroxisome proliferator-activated receptor gamma knockout causes insulin resistance in fat and liver but not in muscle. *Proc. Natl Acad. Sci. USA*, **100**, 15712–15717.
65. Shepherd, P.R. and Kahn, B.B. (1999) Glucose transporters and insulin action—implications for insulin resistance and diabetes mellitus. *N. Engl. J. Med.*, **341**, 248–257.

66. Minokoshi, Y., Kahn, C.R. and Kahn, B.B. (2003) Tissue-specific ablation of the GLUT4 glucose transporter or the insulin receptor challenges assumptions about insulin action and glucose homeostasis. *J. Biol. Chem.*, **278**, 33609–33612.
67. Hammarstedt, A., Andersson, C.X., Rotter Sopasakis, V. and Smith, U. (2005) The effect of PPARgamma ligands on the adipose tissue in insulin resistance. *Prostaglandins Leukot. Essent. Fatty Acids*, **73**, 65–75.
68. Cui, L., Jeong, H., Borovecki, F., Parkhurst, C.N., Tanese, N. and Krainc, D. (2006) Transcriptional repression of PGC-1alpha by mutant huntingtin leads to mitochondrial dysfunction and neurodegeneration. *Cell*, **127**, 59–69.
69. Weydt, P., Pineda, V.V., Torrence, A.E., Libby, R.T., Satterfield, T.F., Lazarowski, E.R., Gilbert, M.L., Morton, G.J., Bammler, T.K., Strand, A.D. *et al.* (2006) Thermoregulatory and metabolic defects in Huntington's disease transgenic mice implicate PGC-1alpha in Huntington's disease neurodegeneration. *Cell Metab.*, **4**, 349–362.
70. Taherzadeh-Fard, E., Saft, C., Andrich, J., Wieczorek, S. and Arning, L. (2009) PGC-1alpha as modifier of onset age in Huntington disease. *Mol. Neurodegener.*, **4**, 10.
71. Chaturvedi, R.K., Adhihetty, P., Shukla, S., Hennessy, T., Calingasan, N., Yang, L., Starkov, A., Kiaei, M., Cannella, M., Sassone, J. *et al.* (2009) Impaired PGC-1alpha function in muscle in Huntington's disease. *Hum. Mol. Genet.*, **18**, 3048–3065.
72. Sherman, M.Y. and Goldberg, A.L. (2001) Cellular defenses against unfolded proteins: a cell biologist thinks about neurodegenerative diseases. *Neuron*, **29**, 15–32.
73. Sun, F., Kanthasamy, A., Anantharam, V. and Kanthasamy, A.G. (2007) Environmental neurotoxic chemicals-induced ubiquitin proteasome system dysfunction in the pathogenesis and progression of Parkinson's disease. *Pharmacol. Ther.*, **114**, 327–344.
74. van Tijn, P., Hol, E.M., van Leeuwen, F.W. and Fischer, D.F. (2008) The neuronal ubiquitin–proteasome system: murine models and their neurological phenotype. *Prog. Neurobiol.*, **85**, 176–193.
75. Mestre, T., Ferreira, J., Coelho, M.M., Rosa, M. and Sampaio, C. (2009) Therapeutic interventions for disease progression in Huntington's disease. *Cochrane Database Syst. Rev.*, CD006455.
76. Hunt, M.J. and Morton, A.J. (2005) Atypical diabetes associated with inclusion formation in the R6/2 mouse model of Huntington's disease is not improved by treatment with hypoglycaemic agents. *Exp. Brain Res.*, **166**, 220–229.
77. Lee, M.J., Chang, C.P., Lee, Y.H., Wu, Y.C., Tseng, H.W., Tung, Y.Y., Wu, M.T., Chen, Y.H., Kuo, L.T., Stephenson, D. *et al.* (2009) Longitudinal evaluation of an *N*-ethyl-*N*-nitrosourea-created murine model with normal pressure hydrocephalus. *PLoS ONE*, **4**, e7868.
78. Ma, M., Basso, D.M., Walters, P., Stokes, B.T. and Jakeman, L.B. (2001) Behavioral and histological outcomes following graded spinal cord contusion injury in the C57Bl/6 mouse. *Exp. Neurol.*, **169**, 239–254.
79. Laemmli, U.K. (1970) Cleavage of structural proteins during the assembly of the head of bacteriophage T4. *Nature*, **227**, 680–685.
80. Chiang, M.C., Juo, C.G., Chang, H.H., Chen, H.M., Yi, E.C. and Chern, Y. (2007) Systematic uncovering of multiple pathways underlying the pathology of Huntington disease by an acid-cleavable isotope-coded affinity tag approach. *Mol. Cell Proteomics*, **6**, 781–797.
81. Wanker, E.E., Scherzinger, E., Heiser, V., Sittler, A., Eickhoff, H. and Lehrach, H. (1999) Membrane filter assay for detection of amyloid-like polyglutamine-containing protein aggregates. *Methods Enzymol.*, **309**, 375–386.
82. Liu, F.C., Wu, G.C., Hsieh, S.T., Lai, H.L., Wang, H.F., Wang, T.W. and Chern, Y. (1998) Expression of type VI adenylyl cyclase in the central nervous system: implication for a potential regulator of multiple signals in different neurotransmitter systems. *FEBS Lett.*, **436**, 92–98.
83. Ehrlich, M.E., Conti, L., Toselli, M., Taglietti, L., Fiorillo, E., Taglietti, V., Ivkovic, S., Guinea, B., Tranberg, A., Sipione, S., Rigamonti, D. and Cattaneo, E. (2001) ST14A cells have properties of a medium-size spiny neuron. *Exp. Neurol.*, **167**, 215–226.
84. Pendergrass, W., Wolf, N. and Poot, M. (2004) Efficacy of MitoTracker Green and CMXrosamine to measure changes in mitochondrial membrane potentials in living cells and tissues. *Cytometry A*, **61**, 162–169.
85. Huntington Study Group. (1996) Unified Huntington's Disease Rating Scale: reliability and consistency. Huntington Study Group. *Mov. Disord.*, **11**, 136–142.